Open access • Posted Content • DOI:10.1101/2021.07.21.453299

Csp1, A Cold-Shock Protein Homolog in Xylella fastidiosa Influences Pili Formation, Stress Response, and Gene Expression — Source link

Wei Wei, L. P. Burbank, T. Sawyer

Institutions: United States Department of Agriculture, Agricultural Research Service, Oregon State University

Published on: 22 Jul 2021 - bioRxiv (Cold Spring Harbor Laboratory)

Topics: Xylella fastidiosa, Virulence and Wild type

Csp1, A Cold-Shock Protein Homolog in *Xylella fastidiosa* Influences Pili Formation, Stress Response, and Gene Expression

Wei Wei[1*], Teresa Sawyer[2], Lindsey P. Burbank[1]

[1]USDA Agricultural Research Service, San Joaquin Valley Agricultural Sciences Center, Parlier, CA

[2]Electron Microscopy Facility, Oregon State University, Corvallis, OR

*Corresponding author: wei.wei2@usda.gov

Abstract

Bacterial cold shock-domain proteins (CSPs) are conserved nucleic acid binding chaperones that play important roles in stress adaptation and pathogenesis. Csp1 is a temperature-independent cold shock protein homolog in Xylella fastidiosa, a bacterial plant pathogen of grapevine and other economically important crops. Csp1 contributes to stress tolerance and virulence in X. fastidiosa. However, besides general single stranded nucleic acid binding activity, little is known about the specific function(s) of this protein. To further investigate the role(s) of Csp1, we compared phenotypic differences between wild type and a csp1 deletion mutant (Δcsp1). We observed decreases in cellular aggregation and surface attachment with the Δcsp1 strain compared to the wild type. Transmission electron microscopy imaging revealed that Δcsp1 had reduced pili compared to the wild type and complemented strains. The Δcsp1 strain also showed reduced survival after long term growth, in vitro. Since Csp1 binds DNA and RNA, its influence on gene expression was also investigated. Long-read Nanopore RNA-Seq analysis of wild type and Δcsp1 revealed changes in expression of several genes important for attachment and biofilm formation in Δcsp1. One gene of intertest, pilA1, encodes a type IV pili subunit protein and was up regulated in Δcsp1. Deleting pilA1 increased surface attachment in vitro and reduced virulence in grapevines. X. fastidiosa virulence depends on bacterial attachment to host tissue and movement within and between xylem vessels. Our results show Csp1 may play a role in both

virulence and stress tolerance by influencing expression of genes important for biofilm formation.

Importance

Xylella fastidiosa is a major threat to the worldwide agriculture industry (1, 2). Despite its global importance, many aspects of *X. fastidiosa* biology and pathogenicity are poorly understood. There are currently few effective solutions to suppress *X. fastidiosa* disease development or eliminate bacteria from infected plants(3). Recently, disease epidemics due to *X. fastidiosa* have greatly expanded(2, 4, 5), exacerbating the need for better disease prevention and control strategies. Our studies show that Csp1 is involved in *X. fastidiosa* virulence and stress tolerance. Understanding how Csp1 influences pathogenesis and bacteria survival can aide in developing novel pathogen and disease control strategies. We also streamlined a bioinformatics protocol to process and analyze long read Nanopore bacterial RNA-Seq data, which has previously not been reported for *X. fastidiosa*.

Introduction

Xylella fastidiosa is an economically important plant pathogen that causes disease in many agricultural crops including grapevines, citrus, almonds, alfalfa, and coffee. Infection of grapevines by *X. fastidiosa* subsp. *fastidiosa* is known as Pierce's disease(6). Pierce's disease is a serious problem for the grapevine industry in the United States, especially in California where the disease threatens the $30 billion wine industry(7). During the infection cycle, *X. fastidiosa* is spread via sap feeding insect vectors and colonizes the xylem tissue of plants(8). In the plant xylem, the bacteria encounter many stressors such as plant defense responses that can reduce pathogen viability. Abiotic stressors such as cold temperature can also affect long-term survival

of the bacteria in grapevines and has been linked to pathogen elimination and vine recovery(9, 10).

Due to its reduced genome size in comparison to other similar bacteria, *X. fastidiosa* lacks some well-developed stress responses, which can reduce cell viability and survival(11). One notable difference is the *X. fastidiosa* genome encodes only two known cold shock protein (Csp) homologs, Csp1 and Csp2(12), while other bacteria like *E. coli* and *Salmonella enterica* have upwards of nine(13–15). Most research on bacterial cold shock proteins have focused on their role in helping bacteria adapt and survive at suboptimal temperatures, however several studies show some Csps also contribute to virulence and general stress response(14, 16–18). In *E. coli*, five of the nine Csps (CspA, CspB, CspE, CspG and CspI) are induced by changes in temperature(15), while CspC and CspE are constitutively expressed at normal growth temperatures (37°C) and are involved in regulating stress response gene expression(13). *E. coli* CspD is induced at early stationary phase and is important for survival under nutrient poor conditions(18). Previous studies on *X. fastidiosa* revealed that Csp1 and Csp2 are not induced by cell exposure to cold conditions (12)(Burbank, unpublished). Data on Csp2 function(s) is limited because attempts to make *X. fastidiosa csp2* deletion mutants were unsuccessful. Deleting *csp1* resulted in reduced survival after cold treatment *in vitro,* however its importance to *X. fastidiosa* cold survival *in planta* is not as well established(12). Csp1 is also important for osmotic stress tolerance(12). These results suggest that like *E. coli* CspE and CspC, *X. fastidiosa* Csp1 may be less important for cold survival and play a more prominent role in general stress tolerance.

In some animal and plant pathogens, Csps are also important for regulation of virulence factors. A triple deletion mutant (Δ*cspABD*) in bacterial foodborne pathogen *Listeria monocytogenes* reduced oxidative and cold stress survival and impaired host cell invasion and

intracellular growth(16). The *L. monocytogenes* Δ*cspABD* mutant was also deficient in cellular aggregation and did not express surface flagella or exhibit swarming motility(19). Gene expression analysis showed reduced expression of virulence and motility genes in *L. monocytogenes csp* mutants, suggesting some Csps may regulate gene expression. Similarly, some cold shock proteins in plant pathogenic bacteria also act as virulence factors and regulate gene expression. The *Xanthomonas oryzae pv. oryzae* (*Xoo*) CspA protein regulates expression of two virulence genes, *PXO_RS11830* and *PXO_RS01060*(17). Deletion of *Xoo cspA* decreased cold tolerance, bacterial pathogenicity, biofilm formation and polysaccharide production(17). In *X. fastidiosa* strain Stag's Leap, deleting *csp1* resulted in significantly reduced disease severity and bacterial titer in the absence of cold stress in susceptible Chardonnay grapevines(12). However, the mechanisms of how Csp1 contributes to stress tolerance and virulence are not well understood.

In this study, we investigated the molecular mechanisms through which *X. fastidiosa* Csp1 contributes to stress tolerance and virulence. Since the *X. fastidiosa csp1* mutant was less tolerant to certain stress conditions and had lower bacterial titer compared to the wild type *in planta*(12), we compared long-term survival of wild type *X. fastidiosa* Stag's Leap with the Δ*csp1* mutant and a complemented strain. We also investigated whether Csp1 influences biofilm formation since xylem occlusion by biofilms is a major aspect of *X. fastidiosa* pathogenicity, and the Δ*csp1* mutant produced less severe symptoms in grapevine compared to the wild type(12). Lastly, because Csp1 has general nucleic acid binding activity(12) and studies in other bacteria show some Csps regulate gene expression, we also investigated the influence of Csp1 on *X. fastidiosa* gene expression using RNA-Seq to compare transcriptomes of wild type Stag's Leap and the Δ*csp1* mutant.

Results

X. fastidiosa Δ*csp1* mutant showed reduced long-term survival *in vitro*

Previous work showed that deleting the *csp1* gene in *X. fastidiosa* strain Stag's Leap resulted in reduced tolerance to salt and cold stress(12). Since these results strongly suggest Csp1 may play a role in *X. fastidiosa* stress adaptation, we were interested if Csp1 was involved in survival under other stresses, such as prolonged growth times. We compared cell viability of wild type, Δ*csp1*, and Δ*csp1/csp1*+ strains grown on PD3 plates at 7 days post inoculation (DPI) when *X. fastidiosa* cells begin to decline, and 13 DPI (extended growth period). No significant change in viability was observed between the mutant and wild-type at 7 days post inoculation (DPI) (Figure 1A), but there was a significant decrease in viability of Δ*csp1* at 13 DPI compared to the wild-type and complemented strains (Figure 1B). These results suggest Csp1 is important for long term survival of *X. fastidiosa in vitro*.

Δ*csp1* strain showed reduced cellular aggregation and surface adhesion

Biofilm formation is an important aspect of *X. fastidiosa* host colonization and involves both cell-cell aggregation and cellular adhesion to surfaces(20). Wild type Stag's Leap cells form visible aggregates and a biofilm ring at the air-liquid interface when grown in liquid PD3 media (Figure 2A). However, the Δ*csp1* mutant showed a dispersed phenotype with visibly less cells attached at the air-liquid interface when grown under the same conditions as WT and the complemented strains (Figure 2A). We quantified and compared aggregation of the WT, Δ*csp1*, and Δ*csp1/csp1*+ strains and found that the percentage of aggregated cells in liquid culture was significantly lower for *Δcsp1* compared to the WT and complemented strains (Fig. 2B). In addition to cellular aggregation, biofilm formation also requires cell adhesion to surfaces. We quantified surface attachment of static cultures of WT, Δ*csp1*, and Δ*csp1/csp1*+ strains grown in

96-well plates using crystal violet staining and observed a significant decrease in the amount of attached cells for the mutant strain compared to WT and the complemented strains (Figure 2C).

Δ*csp1* mutant shows reduced pili formation

X. fastidiosa pili are important for cellular aggregation and surface attachment(21). To evaluate the effect of *csp1* on pilus formation, cells of the wild type Stag's Leap, Δ*csp1* mutant, and the complemented strains were visualized using Transmission electron microscopy (TEM), as shown in Figure 3. TEM images of wild-type *X. fastidiosa* shows pili localized to one pole of the cell, while the *csp1* mutant did not show visible pili formation (Figure 3). The complemented strain shows restored pilus formation, with most of the pili concentrated towards one pole of the cell (Figure 3). TEM was performed at Oregon State University's Electron Microscopy Facility (Corvallis, OR).

Motility and attachment related genes were differentially expressed in the Δ*csp1* strain

To investigate the influence of Csp1 on *X. fastidiosa* gene expression we used Nanopore RNA-Seq to sequence transcriptomes of wild-type *X. fastidiosa* strain Stag's Leap and the Δ*csp1* deletion mutant under standard growth conditions (28°C). RNA-Seq analysis revealed 90 genes were differentially expressed in the Δ*csp1* strain compared to the wild type (Table 1). Of the 90 differentially expressed genes, 65 were down regulated and 25 were up regulated in Δ*csp1* compared to the wild type. The RNA-Seq results also showed that no transcripts mapped to the *csp1* gene in the mutant strain, verifying *csp1* was absent and showing the accuracy of transcript mapping (Table 1). Gene ontology analysis using GSEA Pro (http://gseapro.molgenrug.nl/) showed significant enrichment of genes involved in cell adhesion/attachment, gene regulation, translation, and rRNA binding. To identify genes of interest for further investigation, we focused on genes that may be associated with phenotypes observed in the Δ*csp1* mutant, such as reduced

cellular aggregation and attachment. Several differentially expressed genes encoding proteins involved in attachment, motility and/or biofilm formation included *pilA1* (PD1924), *pilA2* (PD1926), *fimA* (PD0062), *fimC* (PD0061), *hsf*/*xadA* (PD0824), *pilV* (PD0020), and *fimT* (PD1735). We performed qRT-PCR to verify the Nanopore expression data for several of these genes and saw that expression of *pilA1* was consistently up regulated in the *csp1* mutant strain in all samples tested (Supplemental Table 1). Based on these results and findings from other studies showing *pilA1* is involved in *X. fastidiosa* attachment and biofilm formation(22), we chose to investigate the roles(s) of *X. fastidiosa* Stag's Leap *pilA1* further.

Stag's Leap *ΔpilA1* mutant showed increased biofilm formation and decreased cellular aggregation *in vitro*

X. fastidiosa PilA1 is a type IV pili subunit protein that contributes to biofilm formation(22). Studies in *X. fastidiosa* strains TemeculaL and WM1-1 showed deleting *pilA1* leads to overabundance of type IV pili and increased attachment and biofilm formation(22). We observed increased expression of *pilA1* and decreased cell-to-cell adhesion and decreased attachment to surfaces in the Stag's Leap Δ*csp1* mutant, so we created a *pilA1* deletion mutant in the Stag's Leap background to investigate whether PilA1 is involved in attachment and biofilm formation in this strain as well. Similar to Temecula L, the Stag's Leap Δ*pilA1* strain showed an increase in surface attachment compared to the wild type and complemented strains (Figure 4A). The Δ*pilA1* mutant also had reduced cellular aggregation and a dispersed phenotype in liquid media (Figure 4B). TEM images of Stag's Leap Δ*pilA1* show that like the TemeculaL Δ*pilA1* mutant, deleting *pilA1* in Stag's Leap also lead to overabundance of pili distributed around the entire cell (Supplemental Figure S2). These results show that *pilA1* is important for attachment and biofilm formation in Stag's Leap and suggests that the decrease in surface attachment observed in the Δ*csp1* mutant may be a result of increased expression of *pilA1*.

The *ΔpilA1* mutant showed reduced virulence in grapevines

Xylem vessel occlusion caused by biofilms is one major mechanism of *X. fastidiosa* pathogenicity. Previous studies showed the Δ*csp1* mutant is less virulent in Chardonnay grapevines compared to wild type Stag's Leap(12). Since both the Δ*csp1* and Δ*pilA1* mutant strains have altered biofilm phenotypes, and *pilA1* expression is up regulated in the Δ*csp1* strain, we were interested if *pilA1* also influences virulence in grapevines. We inoculated susceptible one-year-old potted Chardonnay grapevines with wild type Stag's Leap, Δ*pilA1*, Δ*pilA1/pilA1+* cultures or 1XPBS as the negative control. Disease severity was significantly reduced for plants inoculated with the *ΔpilA1* strain compared with plants inoculated with wild type and complemented strains at 16 weeks post-inoculation (Fig. 5A). The bacterial populations in inoculated plants were also quantified using qPCR. There was no significant difference in *X. fastidiosa* populations detected in petioles from plants inoculated with *ΔpilA1*, wild type, or the complemented strains at 16 weeks post-inoculation (Fig. 5B). This suggests that the virulence defect of the mutant strain was not due to reduced bacterial populations. Grapevine virulence assays were repeated the following year using the same *X. fastidiosa* strains and disease severity was calculated at 11 weeks post inoculation (11 weeks was used instead of 16 weeks due to time restraints). There was no significant difference in disease severity of grapevines inoculated with the different *X. fastidiosa* strains or the negative control at 11 weeks post inoculation (Supplemental Figure S3).

Discussion

Bacterial Csp homologs are involved in a wide range of functions including cold tolerance, general stress response, and virulence(12, 17, 23). Csps involved in both stress response and virulence have been found in many animal pathogens such as *L.*

187 *monocytogenes*(16, 19), *Brucella melitensis*(24), *Salmonella enterica* serovar Typhimurium(14),
188 *Enterococcus fecalis*(23), *Staphylococcus aureus*(25), as well as plant pathogens *Xanthomonas*
189 *oryzae pv. oryzae*(17) and *X. fastidiosa*(12). Deleting Csp genes in these bacteria resulted in
190 attenuated virulence, sometimes together with changes to cellular aggregation, surface
191 attachment, and biofilm formation(19). However, the functional mechanisms underlying how
192 Csps influence stress response and virulence are not well understood. In this study, we showed
193 that *X. fastidiosa* Csp1 may have a role in regulating gene expression since deleting the *csp1*
194 gene in strain Stag's Leap influenced expression of 90 genes, several of which encode proteins
195 important for bacteria attachment and motility such as the type IV pili gene *pilA1*. The phenotype
196 of the Δ*csp1* mutant supported our transcriptome data, showing changes in cellular aggregation
197 and surface attachment, processes that involve type I and type IV pili(21, 26). TEM images of
198 Δ*csp1* showed a significant reduction in the number of visible pili compared to the wild type and
199 complemented strains. Deleting *csp1* also reduced bacterial viability during late stationary phase,
200 suggesting Csp1 is important for long-term survival.

201 Biofilm formation is an important part of *X. fastidiosa* insect vector and plant
202 colonization(27). Xylem blockage by biofilms restricts water flow and is a major mechanism of
203 *X. fastidiosa* pathogenicity(28). Biofilm development in *X. fastidiosa* is highly regulated and
204 requires surface attachment and cellular aggregation, which are dependent on type I and type IV
205 pili(29). Transcriptome analysis showed decreased expression of type I pilin gene *fimA* and type
206 IV pili genes *pilA2* and *fimT*, while the type IV pili gene *pilA1* was up regulated in the Δ*csp1*
207 mutant. The functions of *fimA*, *pilA2* and *fimT* were not investigated further in this study due to
208 inconsistent gene expression results using quantitative RT-PCR to validate the RNA-Seq data.
209 Other studies showed *X. fastidiosa* mutants lacking *fimA* had aggregation- and biofilm-deficient

phenotypes, but were twitching-enhanced(26, 30), while mutants in *pilA2* were twitching-deficient compared to the wild type(22). Twitching motility allows *X. fastidiosa* to move against xylem flow and colonize tissue beyond the point of inoculation, making it important for virulence and plant colonization(31). Twitching motility of the Δ*csp1* mutant was not examined in this study but would be of interest for future studies to elucidate whether Csp1 influences this type of movement in *X. fastidiosa* and whether or not it contributed to the decreased virulence and bacterial titer observed in this strain. In addition, future experiments investigating *in planta* biofilm formation of the Δ*csp1* mutant can give us a better understanding of how Csp1 influences *X. fastidiosa* plant colonization.

We further investigated the role(s) of the type IV pilin protein PilA1 since qRT-PCR gene analysis for *pilA1* showed consistent up regulation of this gene in the Δ*csp1* strain in all samples tested. Type IV pilin proteins are flexible, filamentous structures mainly composed of a single pilin protein subunit encoded by *pilA* gene(s)(29). Genome analysis of *X. fastidiosa* showed the presence of at least four paralogs of the *pilA* gene(22). Most studies on bacterial type IV pili highlight their importance for twitching motility, however *pilA1* appears to be more involved in surface attachment and biofilm formation(22). When *pilA1* was deleted from the Stag's Leap genome, we observed increased surface attachment and decreased cellular aggregation. Studies in *X. fastidiosa* strain TemeculaL and WM1-1 also showed deleting *pilA1* increased biofilm formation compared to the wild type strain(22). Electron microscopy of the Stag's Leap, TemeculaL(22), and WM1-1(22) Δ*pilA1* mutants showed increased pili abundance with pili distributed around the entire cell, unlike their respective wild type strains which only showed pili localized to one cell pole. In contrast, the Δ*csp1* mutant, which showed up regulation of *pilA1*, appears to be deficient in pili formation compared to wild type Stag's Leap.

The lack of visible pili in Δ*csp1* may contribute to the reduced attachment phenotype observed for this strain, while the increased abundance of type IV pili in the *ΔpilA1* mutants may contribute to increased attachment. Our Stag's Leap Δ*pilA1* mutant was also less virulent in susceptible Chardonnay grapevines. *X. fastidiosa* disease symptom development is strongly correlated with pathogen spread within infected plants(21, 31), so increased surface attachment of the Δ*pilA1* mutant may restrict bacterial spread within the xylem, leading to the reduced virulence phenotype observed. However, there was no significant difference in bacterial titer between Δ*pilA1* and the wild type or complemented strains, suggesting the virulence defect of Δ*pilA1* may not be entirely due to reduced colonization. The *Δcsp1* mutant showed up-regulation of *pilA1* and decreased virulence in grapevines, while the *ΔpilA1* mutant also had reduced virulence in grapevines, indicating that other factors besides increased expression of *pilA1* are contributing to the Csp1-related virulence defect. Other variables that may be affecting virulence include decreased expression of virulence regulators (PD1905/*xrvA* and PD0708) in Δ*csp1*, or reduction in stress survival *in planta*. The functions of XrvA and the putative PD0708 protein in *X. fastidiosa* are still unclear but would be of interest to investigate in the future.

The Stag's Leap Δ*csp1* mutant was less viable at 13 days post inoculation, which is considered late stationary phase of growth for this strain of *X. fastidiosa*, compared to the wild type and complemented strains. Bacteria in stationary phase encounter many stressors including nutrient limitation, accumulation of toxic by-products, and changes in pH, temperature, osmolarity, etc(32). Studies in other bacteria show that several temperature-independent cold shock proteins are involved in stationary phase stress response. *E. coli* CspD, which is 55.2% identical to the *X. fastidiosa* Csp1 amino acid sequence, is expressed during stationary phase upon glucose starvation and oxidative stress(18). The function of CspD is inhibition of DNA

256 replication by nonspecific binding to single-stranded DNA regions at replication forks(33), and
257 deletion of *cspD* leads to deceased persister cell formation while overexpression of *cspD* is lethal
258 in *E. coli*(33). Bacterial persister cells are more resistant to antibiotics and can often be found in
259 biofilm communities(34). Bacteria in biofilms are more resistance to host defense responses and
260 antimicrobial compounds(35, 36), and have increased nutrient availability(37). Copper-based
261 products are often used to control bacterial pathogens in agriculture, and transcriptome studies
262 show that treating *X. fastidiosa* subsp. *pauca* biofilms with copper resulted in up-regulation of
263 genes important for biofilm and persister cell formation including the toxin-antitoxin system
264 MqsR/MqsA[29] which in *E. coli*, regulates expression of *cspD.* The *E. coli* MqsR toxin is also
265 directly involved in biofilm development and is linked to the development of persister cells(38).
266 Overexpression of the *X. fastidiosa* MqsR toxin in a citrus pathogenic strain led to increased
267 biofilm formation and decreased cell movement, resulting in reduced pathogenicity in citrus
268 plants. In *X. fastidiosa* Temecula-1, an *mqsR* deletion mutant had reduced biofilm formation(39).
269 MqsR over production also increased persister cell formation under copper stress in *X.*
270 *fastidiosa*(40). It is unknown whether *csp1* expression in Stag's Leap is regulated or influenced
271 by the MqsR/MqsA complex, however functional similarities between Csp1 and CspD and the
272 results from studies in *E. coli* showing *cspD* is directly regulated by MqsR/MqsA suggest this is
273 a possibility. Future studies looking at possible links between Csp1 and the MqsR/MqsA toxin-
274 antitoxin system can shed more light on *X. fastidiosa* stress tolerance and survival.

275 In summary, Csp1 is important for virulence and stress response in *X. fastidiosa*. Based
276 on data from this study and past studies in *X. fastidiosa* and other bacteria, cold shock proteins
277 like Csp1 may affect both pathogenicity and stress tolerance by influencing expression of genes
278 important for biofilm formation. Biofilm formation is an essential virulence factor for *X.*

fastidiosa and contributes to bacterial stress tolerance. The results of this study highlight the complexity of *X. fastidiosa* pathogen biology and more work looking at how cold shock proteins affect these processes will help us better understand how this pathogen colonizes and causes disease in hosts.

Methods

Bacterial culture conditions. The wild type strain used in this study is *Xylella fastidiosa* subspecies *fastidiosa* strain 'Stag's Leap' isolated from grapevines with Pierce's Disease in California, USA (41). The Δ*csp1* mutant strain used in this study has the *csp1* (PD1380) gene deleted and replaced with a Chloramphenicol resistance cassette(12). For all *in vitro* experiments, *X. fastidiosa* strains were grown on PD3(42) agar plates or liquid PD3 media without antibiotics or supplemented with 5 µg/mL of chloramphenicol and/or gentamycin when needed. *Escherichia coli* strains used for cloning and propagating of plasmid constructs were grown on LB medium supplemented with appropriate antibiotics at the following concentrations: chloramphenicol 35 µg/mL, spectinomycin 100 µg/mL, and gentamycin 10 µg/mL. All bacterial strains and plasmids used in this study are listed in Table 2 and 3, respectively.

Construction of mutant and complemented strains. The *X. fastidiosa ΔpilA1* mutant strain was constructed by replacing the *pilA1* open reading frame with the Chloramphenicol resistance cassette from plasmid pCR8-csp1-chl(12) using homologous recombination. 931 bp of the upstream flanking region of the *pilA1* coding sequence was amplified from the WT Stag's Leap gDNA using the primers pilA1-up-F/pilA1-up-R-SacI (Table 4). The pilA1-up-R-SacI adds a SacI restriction site to the 3' end of the PCR product. 1.3kb of the downstream flanking region of the *pilA1* coding sequence was amplified using primers pilA1-down-F-XbaI/pilA1-down-R (Table 4). The pilA1-down-F-XbaI primer adds the XbaI restriction site to the 5' end of the PCR

product. The chloramphenicol resistance cassette from pCR8-csp1-chl(12) was amplified using primers Chl-F-SacI/Chl-R-XbaI, which adds SacI and XbaI restriction sites to the 5' and 3' ends, respectively, of the Chloramphenicol resistance cassette amplicon. All PCR reactions were performed using the high-fidelity Platinum™ *Taq* DNA Polymerase (Thermo Fisher). The chloramphenicol resistance cassette amplicon was ligated to the *pilA1* upstream and downstream flanking region amplicons using restriction enzyme cloning with SacI and XbaI (New England Biolabs) and T4 DNA ligase (Invitrogen). The ~3.5kb ligation product was cloned into rapid TA cloning vector pCR8/GW/TOPO (Thermo Fisher) following the manufacturer's instructions to create pCR8-ΔpilA1-chl. The TA cloning reaction was transformed into *E.coli* OneShot Top 10 competent cells (Thermo Fisher) and cells were spread onto LB agar supplemented with 100 µg/mL spectinomycin for selection of transformants. Transformants were screened for the correct 3.5kb insert using colony PCR with the primers pilA1-up-F/pilA1-down-R. Five colonies with the correct sized insert were inoculated into liquid LB supplemented with spectinomycin and chloramphenicol and grown overnight at 37°C for plasmid extraction using a QIAprep Spin Miniprep Kit (Qiagen). The plasmid constructs were confirmed by Sanger sequencing. Plasmid pCR8-ΔpilA1-chl was then transformed into WT *X. fastidiosa* using the natural transformation protocol(43) for mutagenesis via homologous recombination. Transformants were selected on PD3 agar supplemented with chloramphenicol and resistant colonies were screened by colony PCR using *X. fastidiosa* specific primers RST31/RST33(44) and gene specific primers to confirm the size of the insertion region (pilA1-ORF-F/pilA1-ORF-R, Table 4). The deletion mutation was confirmed by Sanger sequencing.

For complementation of the *pilA1* deletion, the *pilA1* ORF plus upstream and down stream flanking regions was inserted into the chromosome of the *X. fastidiosa* Δ*pilA1* strain at a

neutral site as described(45). The *pilA1* ORF plus 405 bp of upstream and 215 bp of downstream sequence was PCR amplified from WT Stag' Leap gDNA template using Platinum Taq polymerase and primers pilA1-OFR-405-F/pilA1-ORF-R (Table 4) and TA cloned into pCR8/GW/TOPO to created pCR8-pilA1-ORF (Table 3). Plasmid pCR8-pilA1-ORF was recombined with plasmid pAX1-GW(12) (Table 3) using the Gateway LR recombination protocol (Invitrogen). The resulting plasmid, pAX1-pilA-ORF, was purified from *E. coli* transformants and the correct insertion was confirmed by Sanger sequencing. pAX1-pilA-ORF was naturally transformed into the *X. fastidiosa ΔpilA1* strain, and transformants were selected on PD3 agar plates supplemented with gentamycin. Transformants were screened using colony PCR with *X. fastidiosa*-specific primers (RST31/RST33) and gene specific primers (pilA1-OFR-405-F/pilA1-ORF-R). Complementation inserts were also confirmed by Sanger sequencing.

Cell aggregation assay. *X. fastidiosa* strains were grown on PD3 agar plates and incubated at 28°C for 6-7 days. After incubation, bacteria cells were scraped off plates and resuspended in 5ml of liquid PD3 media (per sample) to OD_{600} = 0.10. Liquid cultures were grown in sterile 15 mL polypropylene test tubes at 28°C without shaking for 6-7 days. At least 3 replicates per strain were included. Cell aggregation was quantified using the OD_{600} of the upper culture (ODs) and the OD_{600} of the total culture (OD_T). ODs, which is composed mostly of dispersed cells, was determined by measuring OD_{600} of undisturbed cultures. OD_T was measured after aggregated cells were dispersed using a pipette and vortexing. The relative percentage of aggregated cells was estimated using the formula: [(ODt - ODs)/ODt] x100(46). The assay was repeated at least three separate times.

Cell attachment assay. All procedures for setting up the attachment assays were performed aseptically. *X. fastidiosa* strains used in the attachment assays were grown on PD3 agar plates

and incubated at 28°C for 6-7 days. After incubation, bacteria cells were scraped off plates and resuspended in 1 mL (per sample) of liquid PD3 medium. Small volumes of the concentrated cell suspensions were pipetted into 5ml (per sample) of fresh PD3 medium until a concentration of OD_{600} = 0.03-0.05 was reached. Aliquots of 100 µl of cell suspensions were added to individual wells of sterile 96-well polystyrene plates with lids (Nunclon, Cat #163320). Of the remaining cell suspension, 1 mL of each sample was transferred into sterile 1.5 mL centrifuge tubes and incubated at 28°C for 4 days (for gDNA extraction and qPCR later). Uninoculated liquid PD3 medium was used as a negative control. To minimize evaporation issues, we did not use wells from the outer most rows and columns of the plates. Plates were double wrapped with parafilm and incubated at 28°C for 4 days. Cell attachment was quantified using crystal violet staining. Media was removed from 96-well plates and the wells were washed three times with distilled water to remove unbound (planktonic) cells. Cells adhering to the sides of individual wells were stained with 100 µl of 0.1% (*w/v*) crystal violet for 25 min at room temperature. Crystal violet solution was removed from wells and wells were washed three times with distilled water. Crystal violet stain retained by attached cells was eluted by adding 100 µl of 30% acetic acid(47) to each well and quantified using a micro plate reader (Tecan Infinite M1000 PRO) at 550nm wavelength. OD_{550} results were normalized to CFU/ml of cells determined by qPCR. For qPCR, 1 ml aliquots of cells were centrifuged at 9000 rpm for three minutes to pellet cells, then frozen at -20°C until DNA extraction. DNA extraction was performed using a DNeasy Blood & Tissue Kit (Qiagen) following the manufacturer's protocol for gram-negative bacteria. DNA was resuspended in 50 µl of sterile DEPC water (Invitrogen). One µl of each DNA sample was used as template for qPCR with Applied Biosystems PowerUp™ SYBR™ Green Master Mix (ThermoFisher) and primers targeting the *X. fastidiosa* chromosome (XfITS145-60F/ XfITS145-

60R, Table 4). Concentration in CFU/ml was determined based on a standard curve of *X. fastidiosa* DNA extracted from samples with known CFU/ml concentrations. Cell attachment assays were repeated three separate times.

Cell viability assay. Wild type, *Δcsp1*, and *Δcsp1/csp1+* strains were grown on PD3 agar plates for 7-13 days at 28°C. Cells were scraped off plates and resuspended in 1XPBS and diluted to OD_{600} = 0.01. One ml aliquots of each sample were reserved for gDNA extraction for cell quantification by qPCR. 90 µl of cell suspensions were added to individual wells of sterile 96-well plates and 10 µl of AlamarBlue Cell Viability reagent (Invitrogen) was mixed into each well. Plates were incubated in the dark at 37°C for 2 hours. Fluorescence was measured at 560 nm excitation/590 nm emission using a Tecan Infinite M1000 Pro plate reader. Cell aliquots reserved for qPCR were centrifuged at max speed for three minutes to pellet cells, then frozen at -20°C until DNA extraction. DNA extraction was performed using a DNeasy Blood & Tissue Kit (Qiagen) following the manufacturer's protocol for gram-negative bacteria. DNA was resuspended in 50 µl of dH_2O. One µl of each DNA sample was used as template for qPCR with Applied Biosystems PowerUp™ SYBR™ Green Master Mix (ThermoFisher) and primers targeting the *X. fastidiosa* chromosome (XfITS145-60F/ XfITS145-60R, Table 4). Concentration in CFU/ml was determined based on a standard curve of *X. fastidiosa* DNA extracted from samples with known CFU/ml concentrations. Fluorescence readings were normalized to CFU/ml.

Transmission Electron Microscopy of *X. fastidiosa*. *X. fastidiosa* cells were grown on modified PW agar (omit phenol red and add 1.8 g/L of bovine serum albumin)(22) for two to three days. 3mm 300 mesh TEM grids were placed directly on bacteria cells growing on agar media for 5 seconds. Grids were immediately placed on a drop of 1.0% phosphotungstic acid for

30 seconds. Excess stain was wicked off the grid and placed in the FEI Helios Nanolab 650 SEM for STEM imaging.

RNA-seq analysis. Bacteria growth conditions: WT Stag's Leap and Δ*csp1* strains were grown on PD3 agar plates for 6 days at 28°C (6 plates per strain). Cells were aseptically harvested from each plate for all strains and immediately frozen on dry ice for RNA extraction later. Three replicates were included per strain, and each replicate sample included cells from two separate plates.

RNA preparation: Total bacterial RNA was extracted from frozen cells using the Trizol extraction method as described. Briefly, 1ml of Trizol (Invitrogen) reagent was added to each sample (in 1.5ml centrifuge tubes) and incubated at room temperature for 5 minutes. Samples were centrifuged to remove debris and the supernatant was transferred into new 1.5 ml tubes. 0.2 mL of chloroform was added to each sample and mixed thoroughly. Samples were centrifuged at 12,000 x g for 15 minutes. Following centrifugation, the colorless upper aqueous phase containing the RNA was transferred into a fresh tube and RNA was precipitated by adding 0.5 mL of room temperature isopropyl alcohol. Samples were incubated at room temperature for 10 minutes and centrifuged at 12,000 x g for 10 minutes. The RNA pellet was washed twice with 1 mL of 75% ethanol. Ethanol was removed and the RNA pellet was air dried and dissolved in DEPC-treated water. Total RNA was quantified using Quant-iT™ RNA Assay Kit (Invitrogen). 5ug of total RNA was treated with DNase I (Thermo Fisher) following the manufacturer's protocol. DNase-treated RNA was re-precipitated using 0.1 volume sodium acetate and 3X volume ethanol. Poly(A) tail was added to the bacterial mRNA using Poly(A) Tailing Kit (Invitrogen) following the manufacturer's protocol. RNA was re-precipitated using sodium acetate and resuspended in DEPC water (TE buffer was not used because EDTA concentrations

as low as 1 mM will inhibit activity of exonuclease used in the next step). Ribosomal RNA was removed using the Lucigen Terminator 5'-Phosphate Dependent Exonuclease kit following the manufacturer's protocol. The reaction was terminated, and the remaining RNA was precipitated using sodium acetate and ethanol. RNA quantity and quality were measured on the Agilent Bioanalyzer 2100 prior to cDNA library synthesis.

Nanopore cDNA library preparation: cDNA library synthesis was performed using the Oxford Nanopore direct cDNA synthesis kit (Oxford Nanopore) following the manufacturer's protocol. All cDNA synthesis-specific reagents and consumables used were included in the kit unless stated otherwise. 250ng of PolyA+ mRNA resuspended in 7.5 µl of nuclease-free water (per sample) was added to DNA LoBind tubes and centrifuged briefly. Reverse transcription and strand-switching were performed by first adding 2.5 µl VNP primer and 1 µl 10mM dNTPs (ThermoFisher) to each mRNA sample and incubating at 65°C for 5 minutes, followed by immediately cooling on ice. In separate tubes, 4 µl of 5X Maxima H Minus RT Buffer (Thermo Fisher), 1 µl RNaseOUT (ThermoFisher), 1 µl Nuclease-free water, and 2 µl Strand-Switching Primer (SSP) were combined and added to the mRNA samples. Samples were incubated at 42°C for 2 minutes, after which 1 µl of Maxima H Minus Reverse Transcriptase (Thermo Fisher) was added each sample. Samples were incubated at 42°C for 90 minutes, followed by heat inactivation of reaction at 85°C for 5 minutes. Residual RNA was digested by adding 1 µl of RNase Cocktail Enzyme Mix (ThermoFisher) to each reverse transcription reaction. Samples were transferred to new 1.5 mL DNA LoBind Eppendorf tubes and cDNA purified using 17 µl of resuspended AMPure XP beads (Agencourt) flowing the manufacturer's protocols. Samples mixed with AMPure XP beads were centrifuged briefly and beads (bound to cDNA) were immobilized to tube walls using a magnetic tube rack. Tubes were kept on the magnetic rack and

the supernatant removed and discarded. The beads were washed twice with 200 µl freshly prepared 70% molecular grade ethanol. Residual ethanol was removed, and bead pellets were air dried briefly (not to the point of the pellet cracking). Tubes were removed from the magnetic rack and bead pellets were resuspend in 20 µl of DEPC water (Invitrogen). Tubes were put back on the magnetic rack to separate the eluate from the AMPure XP beads, and 20 µl of eluate from each sample were transferred into separate 0.2 mL PCR tubes for cDNA second strand synthesis. 25 µl 2X LongAmp Taq Master Mix (New England Biolabs), 2 µl PR2 primer, and 3 µl of DEPC water was added to each 20 µl eluate sample. Thermal cycler conditions were as follows: 94°C for 1 min, 50°C for 1 min, 65°C for 15 mins, hold at 4°C until next step. Samples were transferred into 1.5 mL DNA LoBind tubes and cDNA purified using 40 µl of AMPure XP beads following the same protocol as previously described. Purified cDNA was eluted in 21 µl of DEPC water. 1 µl of purified cDNA was analyzed on the Agilent Bioanalyzer 2100 to check the quality and quantity. End repair and dA-tailing of fragmented cDNA were performed by mixing: 20 µl cDNA sample, 30 µl Nuclease-free water, 7µl Ultra II End-prep reaction buffer (New England Biolabs), and 3 µl Ultra II End-prep enzyme mix (New England Biolabs). Samples were incubated at 20°C for 5 minutes, followed by 65°C for 5 minutes in a thermal cycler. Samples were transferred into 1.5 mL DNA LoBind Eppendorf tubes and purified using 60 µl of AMPure XP beads following the same protocol as before. Samples were resuspended in 22.5 µl of DEPC water and transferred into a clean 1.5 ml Eppendorf DNA LoBind tubes.

Barcode Ligation: Individual cDNA libraries (12 total) were ligated with unique native barcodes (Oxford Nanopore Native Barcode Expansion set 1-12) following the manufacturer's protocols. 22.5 µl of cDNA was combined with 2.5 µl native barcode and 25 µl Blunt/TA Ligase Master Mix (New England Biolabs). Samples were incubated at room temperature for 10 minutes, and

462 barcoded cDNA libraries were purified using 40 µl of AMPure XP beads and resuspended in 26
463 µl DEPC water following the same protocol as used during cDNA library preparation. 1 µl of
464 each sample was quantified using the Quant-iT High-Sensitivity dsDNA Assay Kit (Thermo
465 Fisher). The quantity of cDNA for one replicate sample of WT 28°C was too low and was
466 excluded from further experiments. The barcoded cDNA libraries from the remaining 11 samples
467 were pooled in equal ratios to obtain 700 ng total DNA and final volume adjusted to 50 µl using
468 nuclease free water and loaded into the Nanopore MinION flow cell (FLO-MIN106). The
469 sequencing reaction was run for 23 hours and generated approximately 4.04 million total reads in
470 FAST5 format.

471 Data Analysis: Nanopore FAST5 files were converted into FASTQ files using the basecalling
472 program Guppy(48) . Barcoded samples were demultiplexed using Deepbinner(49). The program
473 Porechop was used to trim off adapter sequences from the demultiplexed FASTQ reads. The *X.*
474 *fastidiosa* Temecula-1 cDNA reference transcriptome
475 (ftp://ftp.ensemblgenomes.org/pub/bacteria/release-
476 44/fasta/bacteria_18_collection/xylella_fastidiosa_temecula1/cdna/) was indexed and FASTQ
477 reads were mapped to the reference using Minimap2(50). After mapping, aligned reads were
478 quantified using Salmon(51). A table summarizing transcript-level estimates for use in
479 differential gene analysis was created using the R package Tximport(52). Differential expression
480 analysis was performed using the R package DESeq2(53). Descriptions of the programs used and
481 web addresses for downloading the source codes are listed in Supplemental Table 2 (S2).

482 **qRT-PCR Gene Expression Analysis.** Quantitative reverse transcriptase PCR (qRT-PCR) was
483 used to confirm gene expression results of several differentially expressed genes of interest from
484 the RNA-Seq experiment, as well as monitor expression of *csp1* during different *X. fastidiosa*

485 growth stages. For RNA extraction to confirm differentially expressed genes, cells were grown
486 under the same conditions as for the RNA-Seq experiment. For *csp1* expression, cells were
487 grown as described in the cell viability assay. Total RNA was extracted as described in the
488 RNA-Seq methods section using the Trizol (Invitrogen) method. gDNA was removed using
489 Baseline Zero DNase (Lucigen) following the manufacturer's protocols and RNA reprecipitated
490 using 0.1 volume of sodium acetate and 2-3 volumes 100% ethanol. Purified RNA was
491 quantified using a Quant-IT RNA Assay kit (Thermo Fisher Scientific). Removal of residual
492 DNA was confirmed by DNA-specific quantification using a Quant-IT dsDNA Broad Range
493 Assay Kit (Thermo Fisher Scientific). For cDNA synthesis, 500 ng of total RNA was reverse
494 transcribed with random primers using an iScript gClear cDNA synthesis kit (BioRad) and
495 including a no-RT and controls for each sample. 1 µl of each cDNA sample was used as template
496 for qPCR using Applied Biosystems PowerUp SYBR Green Master Mix (Thermo Fisher
497 Scientific). *X. fastidiosa dnaQ* gene, which is a stable reference gene in *X. fastidiosa*(54), was
498 used to normalize expression of other target genes. Primer sequences for target genes are listed in
499 Table 4. PCR cycling conditions were based on recommended protocol provided by PowerUp
500 SYBR Green Master Mix and the melting temperature of the different primer sets. Experiments
501 were repeated three independent times and relative gene expression was calculated with BioRad
502 CFX Manager software.

503 **Plant Virulence Assays.** Plant inoculations: Wild type Stag's Leap, Δ*pilA1*, and Δ*pilA1/pilA1+*
504 strains were grown on PD3 agar plates for 5-7 days and then scraped off plates and resuspended
505 in 1XPBS at concentration OD_{600}=0.25 (~$1x10^8$ CFU/mL). Susceptible (cv Chardonnay) one-
506 year-old potted grapevines were inoculated using a pinprick inoculation method(55). Mock
507 inoculations using 1XPBS were used as negative controls. 20 plants were inoculated with wild

type, 15 plants with Δ*pilA1*, 15 plants with Δ*pilA1/pilA1*+, and 10 plants with 1XPBS. Plants were labeled with number codes and placed randomly within a climate-controlled greenhouse. The plants were monitored weekly for development of scorching symptoms. Once disease symptoms began to develop (5 weeks post inoculation for this experiment), plants were given a disease index score between 0-5 based on a rating scale previously developed(55). A disease score of 0 indicates no disease symptoms and a score of 5 represents severe disease symptoms and plant death. Representative images of disease ratings were provided courtesy of Yaneth Barreto-Zavala and included in Supplemental Figure 2 (S2). Plants were rated until 12 weeks post-inoculation. Area under the disease progress curve (AUDPC) was calculated using average disease intensity over time (weeks) with the Agricolae package for R (https://CRAN.R-project.org/package=agricolae). Plant infection assays were conducted during June-September 2020

qPCR Quantification of Bacterial Populations: At 9- and 12-weeks post-inoculation, petiole samples from infected and mock-inoculated plants were collected for DNA extraction and qPCR quantification of *in planta* bacterial populations. 2-3 petiole samples from each plant were pooled, and samples were lyophilized using a FreeZone (LABCONCO) freezer dryer at -80°C for 24-48 hours. Lyophilized samples were pulverized with 3mm Tungsten Carbide beads (Qiagen) using a Tissue Lyser II (Qiagen) for a total of 4 minutes at 30 r/s. One mL of DNA extraction buffer (20mM EDTA, 350mM Sorbitol, 100mM Tris HCL) with 2.5 % polyvinylpyrrolidone was added to each sample and centrifuged at 14,000 rpm for 5 minutes. All centrifugation steps were performed at 4°C. Supernatant was removed, and pellet was washed with an additional 1 mL of DNA extraction buffer and centrifuged for 10 minutes at 14,000 rpm. Supernatant was removed and pellet was re-suspended with 300 µL of DNA extraction buffer,

300 µL of lysis buffer (50Mm EDTA, 2M NaCl, 2% CTAB, 200mM Tris HCl) and 200 µL of 5% sarcosyl. Tubes were incubated for 45 minutes at 65°C and mixed by vortexing every 15 minutes. After incubation 700 µL of chloroform:isoamly alcohol (24:1) was added to each tube and inverted to mix samples. Samples were then centrifuged at 9500 rpm for 5 minutes. The upper phase was transferred to a new tube and 800 µL of phenol:chloroform:isoamly alcohol (25:24:1) was added. Samples were mixed and centrifuged at 9500 rpm for 5 minutes. The upper phase was transferred to a new tube and 1 mL of isopropanol was added to precipitate the DNA. Samples were mixed and centrifuged at 12000 rpm for 15 minutes. Supernatant was removed and pellet was washed with 300 µL of chilled 70% ethanol and dried under a fume hood. DNA was then re-suspended in 50 µL of TE buffer. Samples were diluted 1:10 in sterile dH_2O prior to quantification by qPCR.

For qPCR, 5 µl of DNA was used as template with Applied Biosystems Fast SYBR Green Master Mix and primers targeting the *X. fastidiosa* chromosome (XfITS145-60F/ XfITS145-60R, Table 4). A standard curve for quantification was made with 10-fold dilutions of *X. fastidiosa* DNA extracted from $1x10^8$ CFL/mL cell suspension combined with uninfected grape DNA in a 2:1 ratio. PCR consisted of 95°C for 3 minutes followed by 35 cycles of 95°C for 30 seconds and 60°C for 30 seconds. PCR was performed using a BioRad CFX96 instrument. CFU/ml as determined by qPCR was normalized to total DNA concentration in ng/µl. Total DNA concentration of original samples was determined using Quant-iT™ dsDNA Assay Kit (Thermo Fisher).

Acknowledgments

We would like to thank Brandon Ortega and Nathaniel Luna for technical support and Yaneth Barreto-Zavala for providing the images used for the grapevine symptoms rating scale. We

554 would also like to thank Leonardo De La Fuente and Marcus Merfa for helpful suggestions
555 regarding imaging pili. Funding for this work was from United States Department of Agriculture
556 (USDA) Agricultural Research Service appropriated project 2034-22000-012-00D. Mention of
557 trade names or commercial products in this publication is solely for the purpose of providing
558 specific information and does not constitute endorsement by USDA. USDA is an equal
559 opportunity provider and employer.

560 **Literature Cited**

561 1. Tumber K, Alston J, Fuller K. 2014. Pierce's disease costs California $104 million per year.
562 California Agriculture 68:20–29.

563 2. Schneider K, Werf W van der, Cendoya M, Mourits M, Navas-Cortés JA, Vicent A,
564 Lansink AO. 2020. Impact of *Xylella fastidiosa* subspecies *pauca* in European olives.
565 PNAS 117:9250–9259.

566 3. 2016. Treatment solutions to cure *Xylella fastidiosa* diseased plants. EFSA Journal
567 14:e04456.

568 4. White SM, Navas-Cortés JA, Bullock JM, Boscia D, Chapman DS. 2020. Estimating the
569 epidemiology of emerging *Xylella fastidiosa* outbreaks in olives. Plant Pathology 69:1403–
570 1413.

571 5. Kottelenberg D, Hemerik L, Saponari M, van der Werf W. 2021. Shape and rate of
572 movement of the invasion front of *Xylella fastidiosa* spp. *pauca* in Puglia. Scientific
573 Reports 11:1061.

574 6. Hopkins DL, Purcell AH. 2002. *Xylella fastidiosa*: Cause of Pierce's Disease of Grapevine
575 and Other Emergent Diseases. Plant Disease 86:1056–1066.

576 7. Kyrkou I, Pusa T, Ellegaard-Jensen L, Sagot M-F, Hansen LH. 2018. Pierce's Disease of
577 Grapevines: A Review of Control Strategies and an Outline of an Epidemiological Model.
578 Front Microbiol 9.

579 8. Almeida RPP, Blua MJ, Lopes JRS, Purcell AH. 2005. Vector Transmission of *Xylella*
580 *fastidiosa*: Applying Fundamental Knowledge to Generate Disease Management Strategies.
581 Annals of the Entomological Society of America 98:775–786.

582 9. Ledbetter CA, Chen J, Livingston S, Groves RL. 2009. Winter curing of *Prunus dulcis* cv
583 'Butte,' *P. webbii* and their interspecific hybrid in response to *Xylella fastidiosa* infections.
584 Euphytica 169:113–122.

585 10. Lieth J, Meyer M, Yeo K-H, Kirkpatrick B. 2011. Modeling Cold Curing of Pierce's
586 Disease in *Vitis vinifera* 'Pinot Noir' and 'Cabernet Sauvignon' Grapevines in California.
587 Phytopathology 101:1492–500.

588 11. Gerlin L, Cottret L, Cesbron S, Taghouti G, Jacques M-A, Genin S, Baroukh C. 2020.
589 Genome-Scale Investigation of the Metabolic Determinants Generating Bacterial Fastidious
590 Growth. mSystems 5.

591 12. Burbank LP, Stenger DC. 2016. A Temperature-Independent Cold-Shock Protein Homolog
592 Acts as a Virulence Factor in *Xylella fastidiosa*. MPMI 29:335–344.

13. Phadtare S, Tadigotla V, Shin W-H, Sengupta A, Severinov K. 2006. Analysis of *Escherichia coli* Global Gene Expression Profiles in Response to Overexpression and Deletion of CspC and CspE. J Bacteriol 188:2521–2527.

14. Michaux C, Holmqvist E, Vasicek E, Sharan M, Barquist L, Westermann AJ, Gunn JS, Vogel J. 2017. RNA target profiles direct the discovery of virulence functions for the cold-shock proteins CspC and CspE. PNAS 114:6824–6829.

15. Yu T, Keto-Timonen R, Jiang X, Virtanen J-P, Korkeala H. 2019. Insights into the Phylogeny and Evolution of Cold Shock Proteins: From Enteropathogenic *Yersinia* and *Escherichia coli* to Eubacteria. Int J Mol Sci 20.

16. Loepfe C, Raimann E, Stephan R, Tasara T. 2010. Reduced Host Cell Invasiveness and Oxidative Stress Tolerance in Double and Triple *csp* Gene Family Deletion Mutants of *Listeria monocytogenes*. Foodborne Pathogens and Disease 7:775–783.

17. Wu L, Ma L, Li X, Huang Z, Gao X. 2018. Contribution of the cold shock protein CspA to virulence in *Xanthomonas oryzae* pv. *oryzae*. Mol Plant Pathol 20:382–391.

18. Yamanaka K, Inouye M. 1997. Growth-phase-dependent expression of *cspD*, encoding a member of the CspA family in *Escherichia coli*. J Bacteriol 179:5126–5130.

19. Eshwar AK, Guldimann C, Oevermann A, Tasara T. 2017. Cold-Shock Domain Family Proteins (Csps) Are Involved in Regulation of Virulence, Cellular Aggregation, and Flagella-Based Motility in *Listeria monocytogenes*. Front Cell Infect Microbiol 7:453.

612 20. Caserta R, Takita MA, Targon ML, Rosselli-Murai LK, Souza AP de, Peroni L, Stach-
613 Machado DR, Andrade A, Labate CA, Kitajima EW, Machado MA, Souza AA de. 2010.
614 Expression of *Xylella fastidiosa* Fimbrial and Afimbrial Proteins during Biofilm Formation.
615 Appl Environ Microbiol 76:4250–4259.

616 21. Li Yaxin, Hao Guixia, Galvani CD, Meng Y, Fuente LDLa, Hoch HC, Burr TJY 2007.
617 Type I and type IV pili of *Xylella fastidiosa* affect twitching motility, biofilm formation and
618 cell–cell aggregation. Microbiology 153:719–726.

619 22. Kandel PP, Chen H, Fuente LDL. 2018. A Short Protocol for Gene Knockout and
620 Complementation in *Xylella fastidiosa* Shows that One of the Type IV Pilin Paralogs
621 (PD1926) Is Needed for Twitching while Another (PD1924) Affects Pilus Number and
622 Location. Appl Environ Microbiol 84:e01167-18.

623 23. Michaux C, Martini C, Shioya K, Lecheheb SA, Budin-Verneuil A, Cosette P, Sanguinetti
624 M, Hartke A, Verneuil N, Giard J-C. 2012. CspR, a Cold Shock RNA-Binding Protein
625 Involved in the Long-Term Survival and the Virulence of *Enterococcus faecalis*. Journal of
626 Bacteriology 194:6900–6908.

627 24. Wang Z, Wang S, Wu Q. 2014. Cold shock protein A plays an important role in the stress
628 adaptation and virulence of *Brucella melitensis*. FEMS Microbiology Letters 354:27–36.

629 25. Uppalapati CK, Gutierrez KD, Buss-Valley G, Katzif S. 2017. Growth-dependent activity
630 of the cold shock *cspA* promoter + 5′ UTR and production of the protein CspA in
631 *Staphylococcus aureus* Newman. BMC Research Notes 10:232.

632 26. De La Fuente L, Burr TJ, Hoch HC. 2008. Autoaggregation of *Xylella fastidiosa* Cells Is
633 Influenced by Type I and Type IV Pili. Appl Environ Microbiol 74:5579–5582.

634 27. Koczan JM, Lenneman BR, McGrath MJ, Sundin GW. 2011. Cell Surface Attachment
635 Structures Contribute to Biofilm Formation and Xylem Colonization by *Erwinia*
636 *amylovora*. Appl Environ Microbiol 77:7031–7039.

637 28. Newman KL, Almeida RPP, Purcell AH, Lindow SE. 2003. Use of a Green Fluorescent
638 Strain for Analysis of *Xylella fastidiosa* Colonization of *Vitis vinifera*. Appl Environ
639 Microbiol 69:7319–7327.

640 29. Craig L, Forest KT, Maier B. 2019. Type IV pili: dynamics, biophysics and functional
641 consequences. Nat Rev Microbiol 17:429–440.

642 30. De La Fuente L, Montanes E, Meng Y, Li Y, Burr TJ, Hoch HC, Wu M. 2007. Assessing
643 Adhesion Forces of Type I and Type IV Pili of *Xylella fastidiosa* Bacteria by Use of a
644 Microfluidic Flow Chamber. Appl Environ Microbiol 73:2690–2696.

645 31. Meng Y, Li Y, Galvani CD, Hao G, Turner JN, Burr TJ, Hoch HC. 2005. Upstream
646 Migration of *Xylella fastidiosa* via Pilus-Driven Twitching Motility. Journal of
647 Bacteriology 187:5560–5567.

648 32. Jaishankar J, Srivastava P. 2017. Molecular Basis of Stationary Phase Survival and
649 Applications. Front Microbiol 8.

650 33. Yamanaka K, Zheng W, Crooke E, Wang Y-H, Inouye M. 2001. CspD, a novel DNA
651 replication inhibitor induced during the stationary phase in *Escherichia coli*. Molecular
652 Microbiology 39:1572–1584.

653 34. Wood TK, Knabel SJ, Kwan BW. 2013. Bacterial Persister Cell Formation and Dormancy.
654 Appl Environ Microbiol 79:7116–7121.

655 35. Prosser BL, Taylor D, Dix BA, Cleeland R. 1987. Method of evaluating effects of
656 antibiotics on bacterial biofilm. Antimicrob Agents Chemother 31:1502–1506.

657 36. González JF, Hahn MM, Gunn JS. 2018. Chronic biofilm-based infections: skewing of the
658 immune response. Pathog Dis 76.

659 37. Kurniawan A, Yamamoto T. 2019. Accumulation of and inside Biofilms of Natural
660 Microbial Consortia: Implication on Nutrients Seasonal Dynamic in Aquatic Ecosystems.
661 International Journal of Microbiology 2019:e6473690.

662 38. Kim Y, Wang X, Zhang X-S, Grigoriu S, Page R, Peti W, Wood TK. 2010. *Escherichia*
663 *coli* toxin/antitoxin pair MqsR/MqsA regulate toxin CspD. Environ Microbiol 12:1105–
664 1121.

665 39. Lee MW, Tan CC, Rogers EE, Stenger DC. 2014. Toxin-antitoxin systems *mqsR/ygiT* and
666 *dinJ/relE* of *Xylella fastidiosa*. Physiological and Molecular Plant Pathology 87:59–68.

667 40. Merfa MV, Niza B, Takita MA, De Souza AA. 2016. The MqsRA Toxin-Antitoxin System
668 from *Xylella fastidiosa* Plays a Key Role in Bacterial Fitness, Pathogenicity, and Persister
669 Cell Formation. Front Microbiol 7.

670 41. Chen J, Wu F, Zheng Z, Deng X, Burbank LP, Stenger DC. 2016. Draft Genome Sequence
671 of *Xylella fastidiosa* subsp. *fastidiosa* Strain Stag's Leap. Genome Announc 4.

672 42. 1981. The Prokaryotes: A Handbook on Habitats, Isolation and Identification of Bacteria.
673 Springer-Verlag, Berlin Heidelberg.

674 43. Kandel PP, Almeida RPP, Cobine PA, De La Fuente L. 2017. Natural Competence Rates
675 Are Variable Among *Xylella fastidiosa* Strains and Homologous Recombination Occurs In
676 Vitro Between Subspecies *fastidiosa* and multiplex. MPMI 30:589–600.

677 44. Minsavage G, Thompson C, Hopkins D, Leite R, Stall R. 1994. Development of a
678 Polymerase Chain Reaction Protocol for Detection of *Xylella fastidiosa* in Plant Tissue.
679 Phytopathology 84.

680 45. Matsumoto A, Young GM, Igo MM. 2009. Chromosome-based genetic complementation
681 system for *Xylella fastidiosa*. Appl Environ Microbiol 75:1679–1687.

682 46. Voegel TM, Doddapaneni H, Cheng DW, Lin H, Stenger DC, Kirkpatrick BC, Roper MC.
683 2013. Identification of a response regulator involved in surface attachment, cell-cell
684 aggregation, exopolysaccharide production and virulence in the plant pathogen *Xylella*
685 *fastidiosa*: *Xylella* XhpT response regulator. Molecular Plant Pathology 14:256–264.

686 47. Merritt JH, Kadouri DE, O'Toole GA. 2005. Growing and analyzing static biofilms. Curr
687 Protoc Microbiol Chapter 1:Unit 1B.1.

688 48. Wick RR, Judd LM, Holt KE. 2019. Performance of neural network basecalling tools for
689 Oxford Nanopore sequencing. Genome Biology 20:129.

690 49. Wick RR, Judd LM, Holt KE. 2018. Deepbinner: Demultiplexing barcoded Oxford
691 Nanopore reads with deep convolutional neural networks. PLOS Computational Biology
692 14:e1006583.

693 50. Li H. 2018. Minimap2: pairwise alignment for nucleotide sequences. Bioinformatics
694 34:3094–3100.

695 51. Patro R, Duggal G, Love MI, Irizarry RA, Kingsford C. 2017. Salmon: fast and bias-aware
696 quantification of transcript expression using dual-phase inference. Nat Methods 14:417–
697 419.

698 52. Soneson C, Love MI, Robinson MD. 2016. Differential analyses for RNA-seq: transcript-
699 level estimates improve gene-level inferences. F1000Res 4:1521.

700 53. Love MI, Huber W, Anders S. 2014. Moderated estimation of fold change and dispersion
701 for RNA-seq data with DESeq2. Genome Biology 15:550.

702 54. Zaini PA, Fogaça AC, Lupo FGN, Nakaya HI, Vêncio RZN, da Silva AM. 2008. The Iron
703 Stimulon of *Xylella fastidiosa* Includes Genes for Type IV Pilus and Colicin V-Like
704 Bacteriocins. J Bacteriol 190:2368–2378.

705 55. Roper MC, Greve LC, Warren JG, Labavitch JM, Kirkpatrick BC. 2007. *Xylella fastidiosa*
706 requires polygalacturonase for colonization and pathogenicity in *Vitis vinifera* grapevines.
707 Mol Plant Microbe Interact 20:411–419.

56. Ledbetter CA, Rogers EE. 2009. Differential Susceptibility of *Prunus* Germplasm (Subgenus *Amygdalus*) to a California Isolate of *Xylella fastidiosa*. HortScience 44:1928–1931.

Figures and Tables

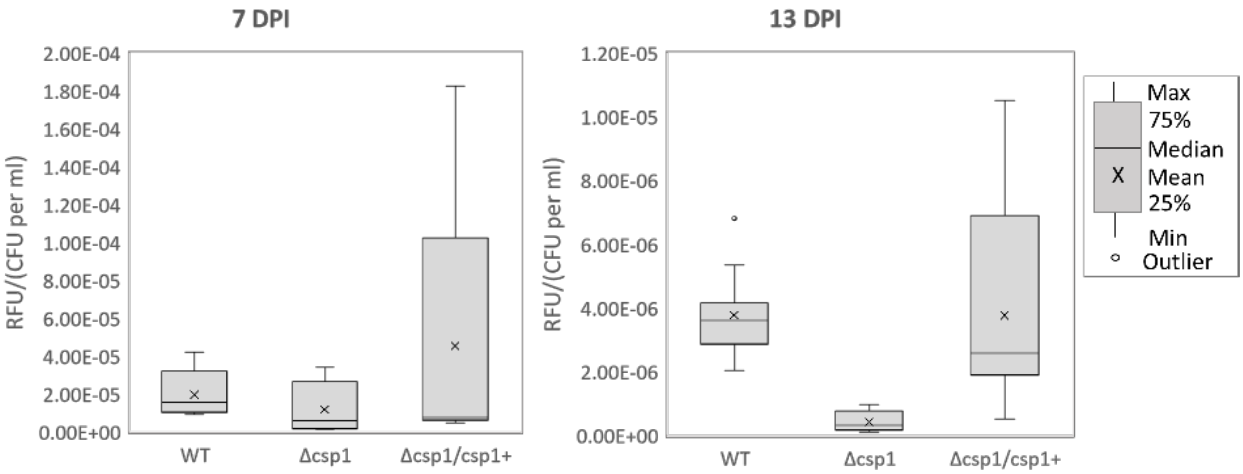

Figure 1. Cell Viability of the Δ*csp1* during long-term growth. Wild type Stag's Leap, Δ*csp1*, and Δ*csp1*/*csp1*+ were grown on PD3 plates for up to 13 days. Cell viability was quantified at 7 days post inoculation (DPI) and 13 DPI using AlamarBlue (Life Technologies) fluorescent cell viability reagent by measuring RFU of each sample and normalizing to total cells quantified by qPCR. Graph represents data collected from at least three independent experiments. **Indicates treatment significantly different from the wild type based on one-way ANOVA followed by Tukey means comparison test ($p<0.01$).

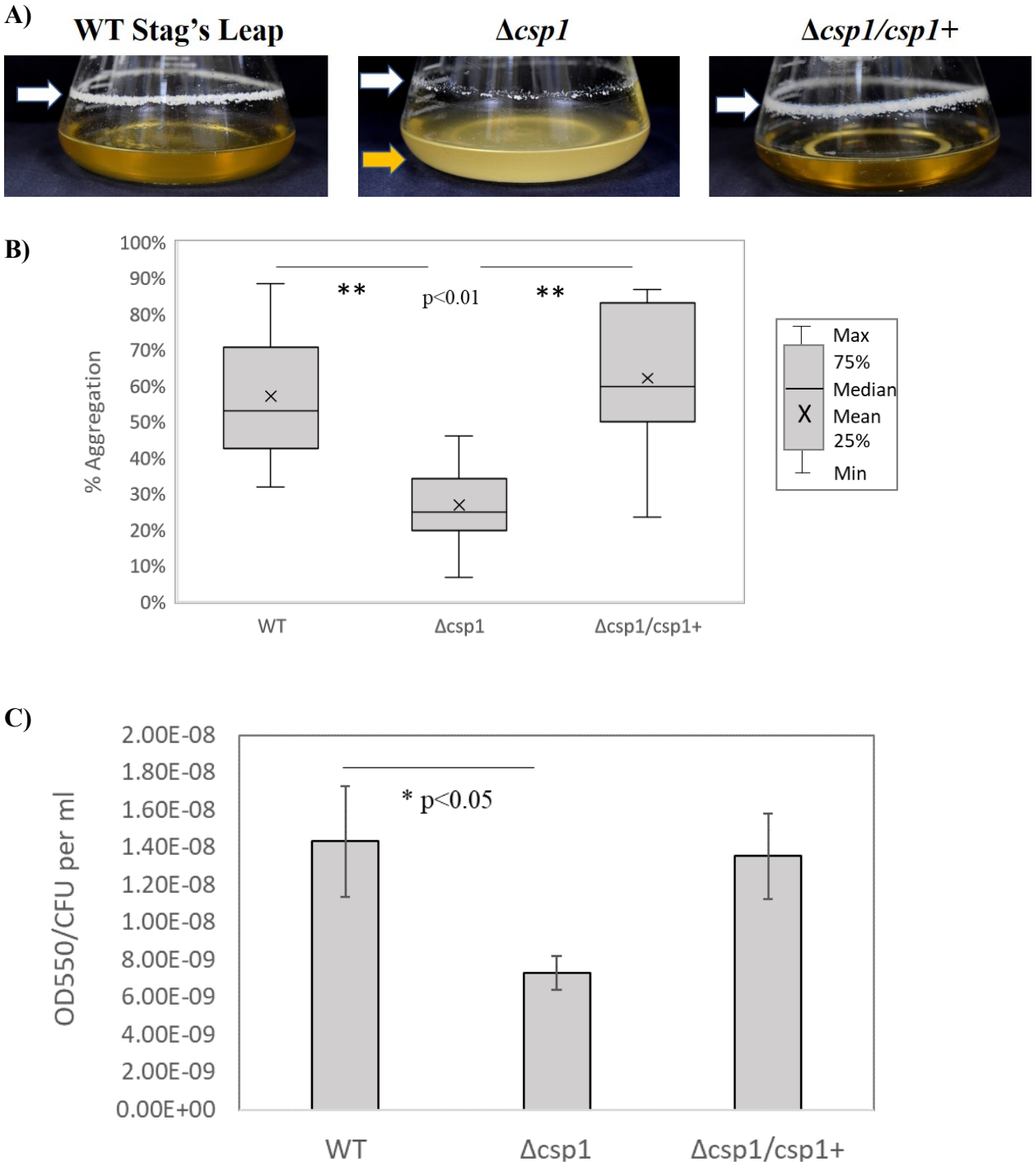

Figure 2. Cellular aggregation and attachment of Δ*csp1*, *in vitro.* A) Cell-cell aggregation and surface attachment was documented after 4 days of growth in liquid PD3 medium at 28°C with shaking at 180 rpm. The yellow arrow indicates the dispersed phenotype of the Δ*csp1*

743 strain, and the white arrows indicate the ring of attached cells at the air-liquid interface. **B)**
744 Cellular aggregation was quantified by measuring the OD_{600} of statically grown liquid cultures of
745 WT, Δ*csp1*, and Δ*csp1/csp1*+ before and after manual dispersal of cells using the equation:
746 $[(OD_{600D}-OD_{600U})/ OD_{600D}]*100$ where OD_{600D} = optical density of dispersed culture and
747 OD_{600U} = optical density of undispersed culture. The graph represents a total of at least nine
748 replicates from three separate experiments. **Indicates significant difference based on one-way
749 ANOVA followed by Tukey means comparison test ($p<0.01$). **C)** Cell attachment was quantified
750 by measuring the amount of crystal violet stain retained by cells attached to the walls of 96-well
751 plates (OD_{550}) after static growth for 4 days. OD_{550} was normalized to total cells (CFU/ml
752 quantified by qPCR). Graph represents at least 45 technical replicates from three separate
753 experiments. *Indicates significant difference ($p<0.05$) from wild type based on one-way
754 ANOVA followed by Bonferroni-Holm.

755

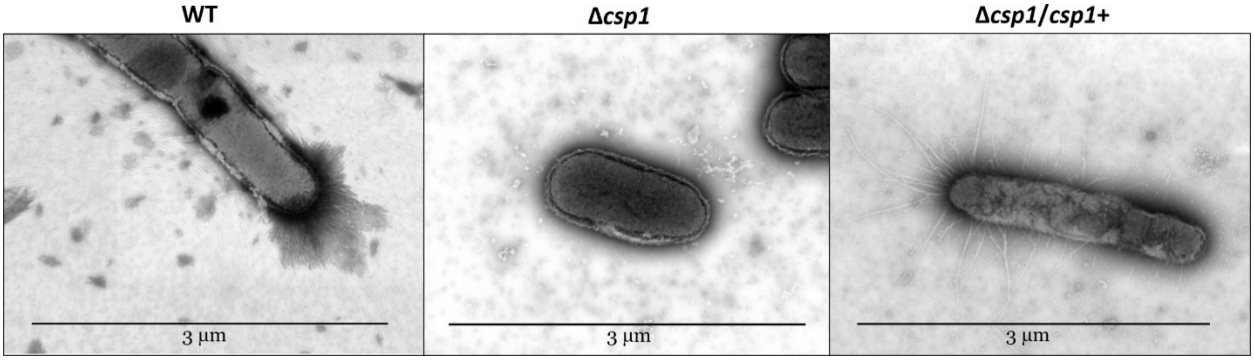

756

757 **Figure 3. TEM images of *X. fastidiosa* strains.** Pili location and abundance were observed for
758 wild type Stag's Leap (WT), the *csp1* mutant (Δ*csp1*), and the complemented (Δ*csp1*/Δ*csp1*+)
759 strains using the Helios NanoLab 650 microscope.

760

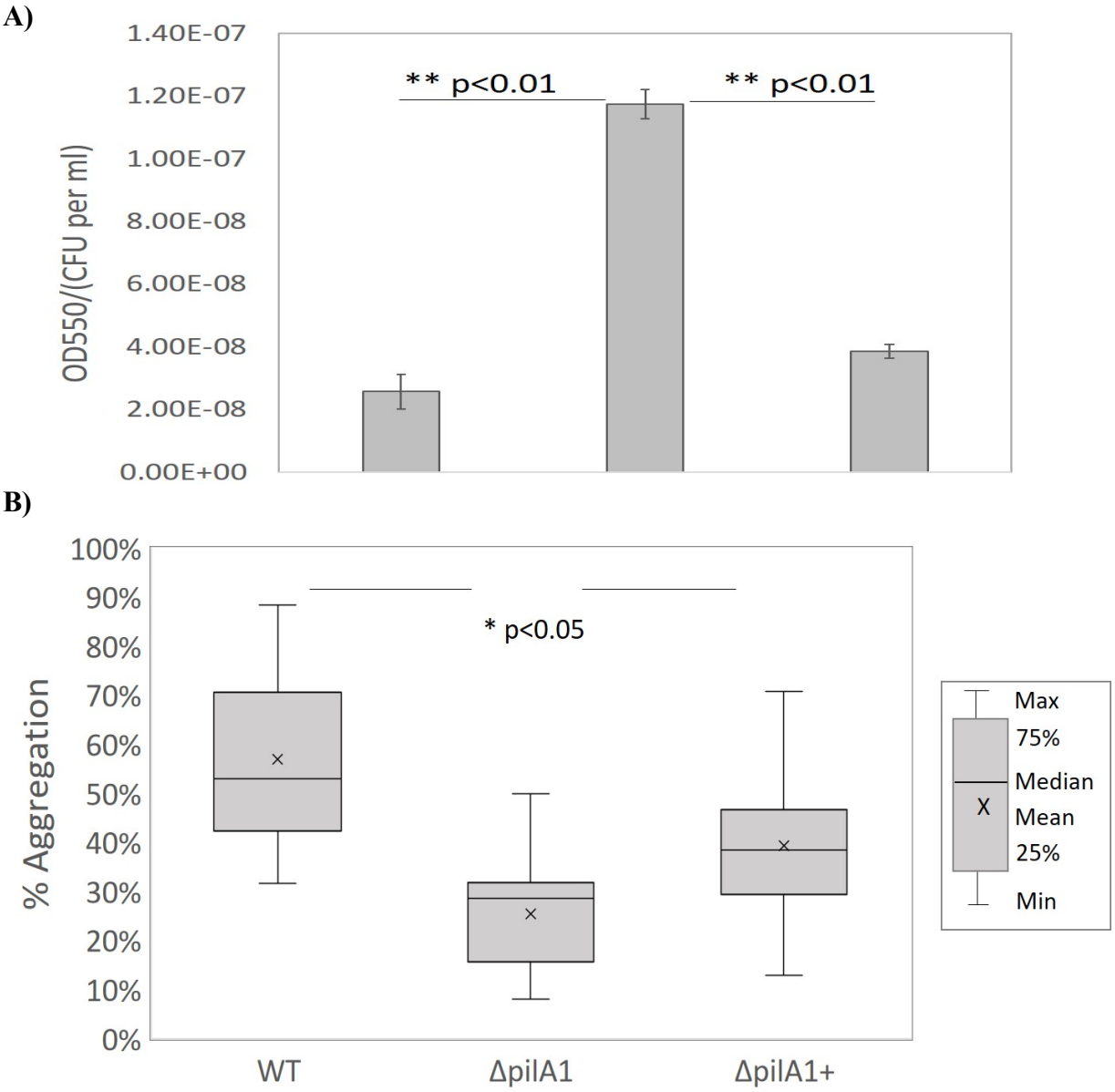

Figure 4. Cellular aggregation and attachment of Δ*pilA1*. A) Cell attachment of wild type Stag's Leap (WT), *pilA1* deletion mutant (Δ*pilA1*)and *pilA1* complemented strain (Δ*pilA1*/*pilA1*+) was quantified by measuring the amount of crystal violet stain retained by cells attached to the walls 15ml polystyrene culture tubes (OD_{550}) after static growth in 5ml of PD3 liquid media for 7 days. OD_{550} was normalized to total cells (CFU per ml) quantified by qPCR. Graph represents at least 16 technical replicates from four separate experiments. **Indicates significant difference from wild type based on one-way ANOVA followed by Tukey means

comparison test ($p<0.01$). **B)** Cellular aggregation was quantified by measuring the OD_{600} of statically grown liquid cultures of WT, Δ*pilA1*, and Δ*pilA1/pilA1+* before and after manual dispersal of cells. The percentage of aggregated cells was calculated using the equation from Figure 2B. The graph represents a total of at least 9 technical replicates from three separate experiments. *Indicates significant difference based on one-way ANOVA followed by Tukey means comparison test ($p<0.05$).

A)

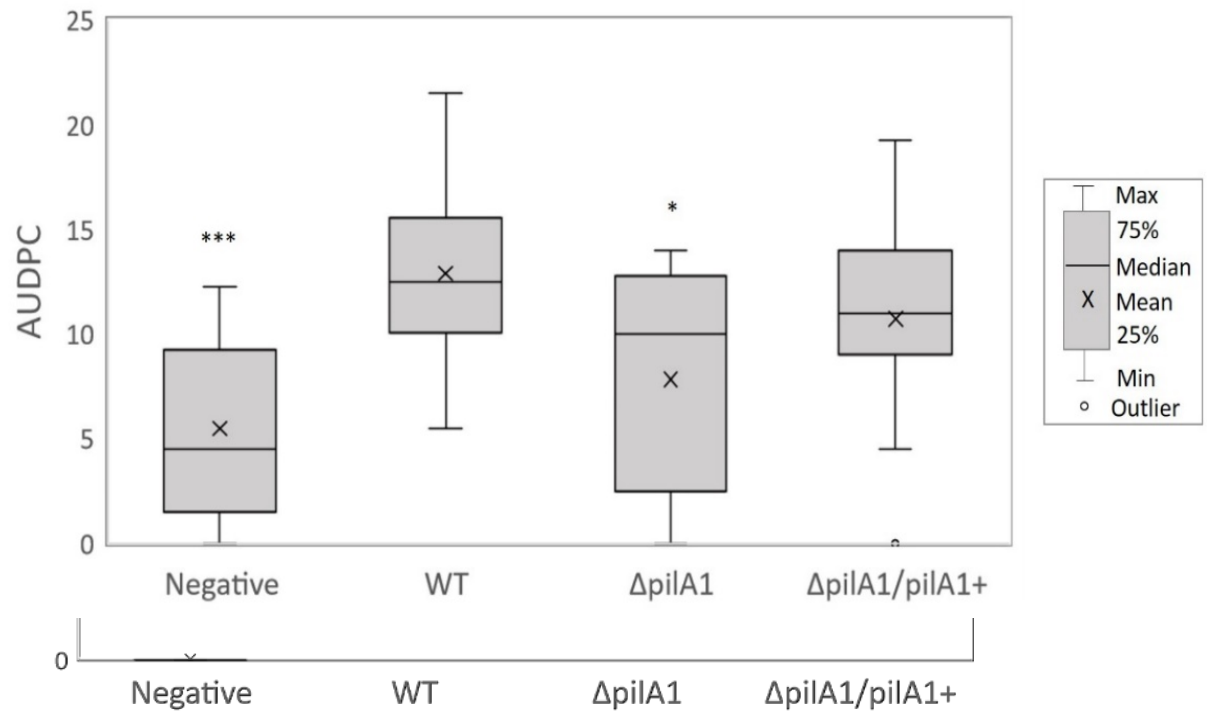

Figure 5. *ΔpilA1* has reduced symptom development in grapevines. One-year old potted grapevines (cv Chardonnay) were mechanically inoculated with wild type Stag's Leap (WT), *pilA1* deletion mutant (Δ*pilA1*), the complemented (Δ*pilA1/pilA1+*) strain, or 1XPBS as the negative control. **A)** Symptom development in grapevines was scored on a 0-5 scale with 0 = no symptoms and 5 = plant death, over the period of 5-16 weeks post-inoculation. Area under the

disease progress curve (AUDPC) was calculated using the Agricolae package for R. **B)** Bacterial populations in plant tissue were quantified using qPCR after 16 weeks post-inoculation and normalized to total DNA concentration. Graphs represents data from 20 plants inoculated with wild type, 15 plants inoculated with Δ*pilA1*, 15 plants inoculated with Δ*pilA1/pilA1*+, and 10 negative control plants. *Indicates treatment significantly different from the wild type based on one-way ANOVA followed by Tukey means comparison test (*= $p<0.05$, **= $p<0.01$, ***=$p<0.001$).

Table 1. Differentially Expressed Genes

			Transcripts per million		
Locus ID	**Gene symbol**	**Product**	**WT**	**Δcsp1**	**Expression Ratio (Δcsp1/WT)**
PD0020	*pilV*	pre-pilin leader sequence	180.08	0.00	0.00
PD0141	*fabG*	3-ketoacyl-(acyl-carrier-protein) reductase	127.23	0.00	0.00
PD1354		hypothetical protein	2582.82	0.00	0.00
PD1380	*csp1*	cold shock protein	5290.81	0.00	0.00
PD1701	*dnaB*	replicative DNA helicase	44.29	0.00	0.00
PD1735	*fimT*	type 4 fimbrial biogenesis protein	131.92	0.00	0.00
PD1944	*rpsR*	30S ribosomal protein S18	8011.60	0.00	0.00
PD2095		hypothetical protein	119.23	0.00	0.00
PD1926	*pilA2*	fimbrial protein	2184.57	66.44	0.03
PD0216	*cvaC*	colicin V precursor	10631.85	842.10	0.08
PD1931	*sucD*	succinyl-CoA synthetase subunit alpha	133.48	11.68	0.09
PD1317		hypothetical protein	112.39	10.34	0.09
PD1905	*xrvA*	virulence regulator	492.63	46.72	0.09
PD2003	*rplJ*	50S ribosomal protein L10	479.16	45.72	0.10
PD0463		hypothetical protein	2108.37	201.98	0.10
PD0084	*rplS*	50S ribosomal protein L19	947.68	115.89	0.12
PD1945	*rpsF*	30S ribosomal protein S6	1201.60	179.24	0.15
PD1063		hypothetical protein	1287.41	202.47	0.16
PD0556		hypothetical protein	28667.31	4555.29	0.16
PD0062	*fimA*	fimbrial subunit precursor	10009.57	1724.44	0.17
PD0217		hypothetical protein	2815.96	511.29	0.18

			Transcripts per million		
Locus ID	**Gene symbol**	**Product**	**WT**	**Δcsp1**	**Expression Ratio (Δcsp1/WT)**
PD1440	*rpsT*	30S ribosomal protein S20	6060.28	1246.99	0.21
PD0708		virulence regulator	672.31	141.02	0.21
PD1914	*rpmI*	50S ribosomal protein L35	21603.77	4619.53	0.21
PD0626	*ssb*	single-stranded DNA-binding protein	484.98	103.71	0.21
PD0061	*fimC*	chaperone protein precursor	477.40	108.95	0.23
PD1087		hypothetical protein	2361.29	585.51	0.25
PD0283	*dksA*	DnaK suppressor	927.35	238.22	0.26
PD0313	*pspB*	serine protease	76.39	19.88	0.26
PD0459	*rpsK*	30S ribosomal protein S11	2578.30	684.46	0.27
PD0460	*rpsD*	30S ribosomal protein S4	949.37	255.44	0.27
PD1913	*rplT*	50S ribosomal protein L20	2372.81	665.13	0.28
PD0447	*rplN*	50S ribosomal protein L14	2169.26	615.27	0.28
PD2122	*rnpA*	ribonuclease P	1479.05	424.04	0.29
PD2121	*yidC*	putative inner membrane protein translocase component YidC	96.10	30.18	0.31
PD0453	*rplR*	50S ribosomal protein L18	1681.26	541.74	0.32
PD1684		hypothetical protein	15592.41	5202.73	0.33
PD0462	*rplQ*	50S ribosomal protein L17	1407.81	481.26	0.34
PD0458	*rpsM*	30S ribosomal protein S13	2889.36	991.26	0.34
PD1557	*apbE*	thiamine biosynthesis lipoprotein ApbE precursor	132.21	46.45	0.35
PD1807	*ompW*	outer membrane protein	3923.03	1396.21	0.36
PD0442	*rplV*	50S ribosomal protein L22	2512.05	900.32	0.36
PD0856	*dcp*	peptidyl-dipeptidase	111.54	42.17	0.38
PD1808		hypothetical protein	35966.82	13605.11	0.38
PD0824	*hsf/xadA*	afimbrial adhesin surface protein	43.10	16.51	0.38
PD0464	*comM*	competence-related protein	257.79	98.85	0.38
PD1993	*csp2*	temperature acclimation protein B	97359.93	38394.08	0.39
PD0246	*secG*	preprotein translocase subunit SecG	1557.96	650.10	0.42
PD0436	*rpsJ*	30S ribosomal protein S10	7969.22	3538.88	0.44
PD1984	*gacA*	transcriptional regulator	694.76	310.36	0.45
PD0448	*rplX*	50S ribosomal protein L24	2529.90	1134.00	0.45
PD1558	*comE*	DNA transport competence protein	16765.37	7555.53	0.45
PD1709	*mopB*	outer membrane protein	597.52	309.74	0.52
PD2123	*rpmH*	50S ribosomal protein L34	36412.20	19544.34	0.54
PD0446	*rpsQ*	30S ribosomal protein S17	11515.54	6378.49	0.55
PD0451	*rpsH*	30S ribosomal protein S8	3394.73	1983.09	0.58

			Transcripts per million		
Locus ID	**Gene symbol**	**Product**	**WT**	**Δcsp1**	**Expression Ratio (Δcsp1/WT)**
PD0060	*fimD*	outer membrane usher protein precursor	75.88	46.68	0.62
PD0452	*rplF*	50S ribosomal protein L6	1627.21	1022.85	0.63
PD0461	*rpoA*	DNA-directed RNA polymerase subunit alpha	477.69	301.63	0.63
PD0159		hypothetical protein	1722.76	1188.73	0.69
PD1506		hemolysin-type calcium binding protein	44.91	33.05	0.74
PD0443	*rpsC*	30S ribosomal protein S3	1071.77	882.49	0.82
PD0437	*rplC*	50S ribosomal protein L3	902.22	780.56	0.87
PD2001	*rpoB*	DNA-directed RNA polymerase subunit beta	132.27	117.96	0.89
PD0444	*rplP*	50S ribosomal protein L16	2534.48	2298.26	0.91
PD1467		hypothetical protein	33.00	104.77	3.18
PD0887	*ruvA*	Holliday junction DNA helicase RuvA	185.24	613.78	3.31
PD0718	*nodQ*	bifunctional sulfate adenylyltransferase subunit 1/adenylylsulfate kinase protein	96.67	322.35	3.33
PD1589	*btuB*	TonB-dependent receptor	21.48	86.50	4.03
PD0179		hypothetical protein	21.64	92.00	4.25
PD1652	*recB*	exodeoxyribonuclease V beta chain	4.63	19.88	4.29
PD1167	*ugd*	UDP-glucose dehydrogenase	41.30	177.84	4.31
PD1924	*pilA1*	fimbrial protein	202.45	892.96	4.41
PD1702		hypothetical protein	80.27	362.95	4.52
PD0744	*hsf*	surface protein	22.05	114.75	5.20
PD1829	*xylA*	family 3 glycoside hydrolase	4.24	22.78	5.37
PD1703		hypothetical protein	82.67	492.01	5.95
PD0405	*rpfG*	response regulator	44.40	271.61	6.12
PD0292	*argE*	acetylornithine deacetylase	13.64	89.63	6.57
PD1517		hypothetical protein	52.15	349.41	6.70
PD1280	*hspA*	low molecular weight heat shock protein	832.27	5951.42	7.15
PD1409	*grx*	glutaredoxin-like protein	76.86	559.19	7.28
PD0521		hypothetical protein	946.01	7042.88	7.44
PD1850		M20/M25/M40 family peptidase	13.43	107.39	7.99
PD1531		hypothetical protein	538.53	5090.18	9.45
PD1468	*bolA*	morphogene BolA protein	236.76	2306.64	9.74

			Transcripts per million		
Locus ID	**Gene symbol**	**Product**	**WT**	**Δcsp1**	**Expression Ratio (Δcsp1/WT)**
PD1392	*gumF*	GumF protein	13.10	233.62	17.83
PD1222		hypothetical protein	321.58	12183.51	37.89
PD0657		hypothetical protein	70.31	2857.66	40.65
PD0215	*cvaC*	colicin V precursor	1211.81	105871.34	87.37

807

808 **Table 2. Bacterial strains**

Strains	**Description**	**Source**
Xylella fastidiosa subspecies *fastidiosa* Stag's Leap	Wild type strain, used to create mutant	(41)
Xf Δcsp1	*X. fastidiosa* deletion mutant in *csp1* (PD1380), Cm^R	(12)
Xf Δcsp1/csp1+	Complemented strain, constructed by chromosomal insertion of *csp1* ORF at neutral site, Cm^R, Gm^R	(12)
Xf ΔpilA1	*X. fastidiosa* deletion mutant in *pilA1* (PD1924), Cm^R	This study
Xf ΔpilA1/pilA1+	Complemented strain, constructed by chromosomal insertion of *pilA1* ORF at neutral site, Cm^R, Gm^R	This study
One Shot® TOP10 Chemically Competent *E. coli*	Commercially available *E. coli* strain used for propagating plasmid constructs, genotype: F- *mcrA* Δ(*mrr-hsd*RMS-*mcr*BC) Φ80*lac*ZΔM15 Δ *lac*X74 *rec*A1 *ara*D139 Δ(*araleu*)7697 *gal*U *gal*K *rps*L (StrR) *end*A1 *nup*G	Invitrogen

809

810 **Table 3. Plasmids**

Plasmid	**Description**	**Source**
pCR8/GW/TOPO	Commercially available cloning vector with 3'-T overhangs. Compatible with Gateway® destination vectors, Sp^R	Invitrogen

pCR8-ΔpilA1-chl	*pilA1* gene deletion construct containing chloramphenicol resistance marker flanked by ~1.5kb upstream and downstream sequences of *pilA1* gene, *pilA1* ORF is deleted, Sp^R, Cm^R	This study
pCR8-pilA1-ORF	*pilA1* complementation construct containing the *Xf pilA1* OFR and flanking regions. Used with Gateway pAX1-GW destination vector, Sp^R	This study
pAX1-GW	Gateway® destination vector used for *Xf* chromosomal gene complementation into neutral location via homologous recombination, Cm^R, Gm^R	(45)
pAX1-pilA1-ORF	Gateway® complementation construct with ORF of *Xf pilA1* and flanking regions, Gm^R	This study

811

812 **Table 4. Primers**

Primer Name	Sequence 5' -> 3'	Source
RST31	GCGTTAATTTTCGAAGTGATTCGATTGC	(44)
RST33	CACCATTCGTATCCCGGTG	(44)
pilA1-up-F	GCCTTGCGAATTTTTCCC	This study
pilA1-up-R-SacI	GGGGAGCTCGTGTATACCTTCAATAAAAAGTTTGGT	This study
pilA1-down-F-XbaI	CCCTCTAGATGAATACACACAGCAACACGATCAATG	This study
pilA1-down-R	AATCGTGTTGTTGCTGGTG	This study
pilA1-ORF-405F	CCGCAGTACGTGTTGC	This study
pilA1-ORF-R	GTTGTAACGGCTCACTC	This study
XfITS145-60F	TACATCGGAATCTACCTTATCGTG	(56)
XfITS145-60R	ATGCGGTATTTAGCGTAAGTTTC	(56)
csp1-qPCR-F	TGATGGGACTCCCGAGGTAT	(12)

csp1-qPCR-R	GGCCTTCATGCAAACTACGG	(12)
PD1924-qRT-F (pilA1)	TATGTTGCCAGATCCCAAGTC	This study
PD1924-qRT-R (pilA1)	TCACCTGAGAATTGCCCTTAAT	This study
dnaQ-qPCR-F	CGTTATCCGGGTCAGCGTAA	(54)
dnaQ-qPCR-R	GTAACTGACGGTGGGCGTTA	(54)

813